POLITECNICO
MILANO 1863

SCUOLA DI INGEGNERIA INDUSTRIALE
E DELL'INFORMAZIONE

BWRs fuel rod steady state thermal analysis

Multiphase Systems and Technologies MSc in Energy/Nuclear Engineering

Davide Marchesi , e-mail : davide4.marchesi@mail.polimi.it

Advisor:
Prof. Colombo Luigi P.M.

Academic year:
2022-2023

Abstract: In this paper is presented a flow boiling thermal analysis of a 'boiling water reactor (BWR)' fuel rod in steady state condition. Data published on Ref [6] relative to the 'Nine Mile Point 2 General Electric BWR-5 with GE11 fuel' were used. All simulations were implemented in MATLAB. The work can be subdivided in two parts : the first part is focused on the characterization of the heat transfer phenomena at nominal power condition and on the description/discussion of the numerical results obtained adopting the various presented correlations. The second part deals with the critical heat flux, the way it occurs (dryout/departure from nucleate boiling) and how it evolves with different steady state operational conditions. All the scripts used for the simulations are open source and easily accessible on the GitHub repositories of the author at the following link.

Key-words: BWR; fuel rod; two phase; flow boiling; CHF; dryout; CPR.

Introduction

Differently from Pressurized water reactors (PWRs), BWRs are characterized by the boiling of the coolant (water) inside the core, from where the generated vapour is directly sent to the turbine, forming in this way a Rankine cycle. This particular design leads the two-phase heat transfer mechanisms to have a central role in many aspects such as the ´neutrons economy', reactor's power production, safety limits and regulations. Due to the importance of this field, usually very precise and detailed studies are conducted through complex CFD or coupled neutronic/thermal-hydraulic numerical simulations. These codes' results are essential especially when dealing with transients and/or accidental conditions. Nuclear reactors are also a unique technology which tend to remain in steady state conditions during almost all the fuel life cycles time. This study has the aim to analyze in a simpler, averaged way, the reactor's thermal-hydraulic's principles, using only MATLAB numerical simulations and two-phase heat transfer correlations. Is given an overview of the characteristics of the operational condition in which the reactor is set, of the limits that are encountered and that must be respected in terms of CHF, and about how they can be managed. All the analysis are carried out considering nominal operational conditions for the ´Nine Mile Point 2 General Electric BWR-5 with GE11 fuel'. Though the approach is very general, good results are obtained simply by changing the values present on the MATLAB script.

List of Symbols			
c_p	specific heat at constant pressure	k	thermal conductivity
p_c	critical pressure	L	length
p_r	reduced pressure	m	mass flow
ΔT_{sat}	surface superheat , $T_w - T_{sat}$	M	molar mass
ΔT_{sub}	liquid subcooling , $T_{sat} - T_f$	Nu	Nusselt number
A	area	p	pressure
Bo	boiling parameter	Pr	Prandtl number
Co	convecitve parameter	$\dot{q}$	rod thermal power
CPR	critical power ratio	q'	rod linear heat
D	diameter	q''	rod heat flux
F	flow factor	Re	Reynolds number
f	friction factor	S	suppression factor
G	mass flux	T	temperature
h	enthalpy	x	vapour quality
	Greek Symbols		
α	heat transfer coefficient	μ	viscosity
ρ	density	σ	bubbles surface tension
	Subscripts		
b	bulk	nb	nucleate boiling
CHF	critical heat flux	ONB	onset of nucleate boiling
g	gas alone	sb	saturated boiling
l	liquid alone	scb	subcooled boiling
go	gas only	w	wall
lo	liquid only	z	axial position

1. Geometries, Fluid Properties and Operational Conditions

The aim of this section is to present the geometries and the physical characteristics considered for the analysis.

1.1. Geometries

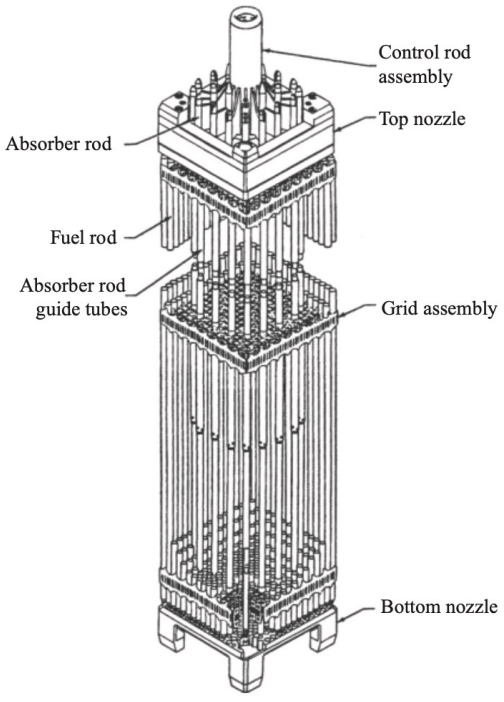

Figure 1: Ref [6] image of an entire LWR fuel assembly

The geometry is the one typical of light water reactor's fuel assembly. The bundle is in vertical position inside the core, and the coolant enters from the lower part of it and passes inside the channels between one fuel rod and the other, to then go upward, being heated, and sent to the turbine. In fig. 1 can be seen the typical configuration. In fig. 2 is represented the cross section of the fuel rods that form it, to better visualize the channel into which the water flows. Like the figure suggests the flow of the coolant inside the core could be divided in many different parts, everyone related to a single rod. This approach was the one adopted to develop the paper. It is considered only a fraction of coolant that could be linked to a single fuel rod, and is not considered the water' flow between one channel and the other. (Note that considering from another point of view, the fraction of the coolant as the one in a channel with the relative four rods surrounding it, would be the same).

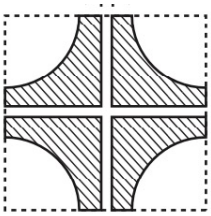

Figure 2: Ref [6] section view of the assembly. The striped part represents the flowing area while the white parts the fuel rods.

Geometrical data			
Pitch	14.37 mm	D_{rod}	11.20 mm
L_{rod} (heated)	3.6 m	A_{flow}	$1.42{*}10^{-4}\ m^2$
Wetted perimeter	πD_{rod}	D_{hyd}	$4\frac{A_{flow}}{\text{wetted perimeter}}$

1.2. Fluid Properties and Operational Conditions

The operational condition is the one relative to the reactor nominal power. The dataset is taken from Ref. [6] and can be seen in the table below.

Nominal operational parameters			
P_{nom}	7.14 MPa	T_{in}	$278.3°C$
m	0.223 kg/s	G_{flow}	1569.5 $\frac{kg}{m^2 s}$
q'_0	47.24 kW/m	Q (reactor total)	3323 MWth

For what concerns the physical properties of water, they are calculated standing on the set parameters above, using the MATLAB script open source function **XSteam** (Ref. [3]). Fluid properties are either re-evaluated at every step z of the axial length during the simulation, or considered as set, in a reasonable way, minimizing as possible both the impact on the simulation results and on the computational weight of the script. Also it must be noted that this study does not take into account a radial discretization, thus all the water properties are bulk averaged. In addition to this, pressure drops are not cosidered.

The heating power of the rod is modeled with a simplified approach with a cosinusoidal function. Considering the linear heat ($\frac{W}{m}$)

$$q'(z) = q'_0 \cos(\frac{\pi z}{L_{rod}}); \qquad q''(z) = \frac{q'(z)}{\pi D_{rod}}. \tag{1}$$

Where the parameter z ranges from -1.8 m to 1.8 m and $z = 0$ is the center of the rod. This means that the actual absolute position Z starting from the first heated point to the last one can be easily calculated as: $Z = z + 1.8$ (m).
The power profile is graphed in fig. 3. The maximum is actually the one set by the parameter q'_0. It must be observed that the heat is zero both at the beginning and at the end of the length of the rod. This, because an additional little simplification was made following the suggestions of Ref. [6] , assuming that the spread of the neutrons inducing the fission events is only limited within the actual heated length of the rod.

2. Correlations

In this section are introduced all the correlations evaluated for the case study. In this part each one will be characterised from the mathematical and physical aspect. All the results and discussions are made in the next sections. When not explicited, the reference (for almost all of them) is Ref [6].

2.1. Subcooled Liquid One Phase Flow

In this condition the **Dittus-Boelter** correlation was used, whose range of applicability actually fits well with our case study ($Re > 10000$, $0.7 < Pr < 100$) . All the liquid properties are calculated at each length z as bulk

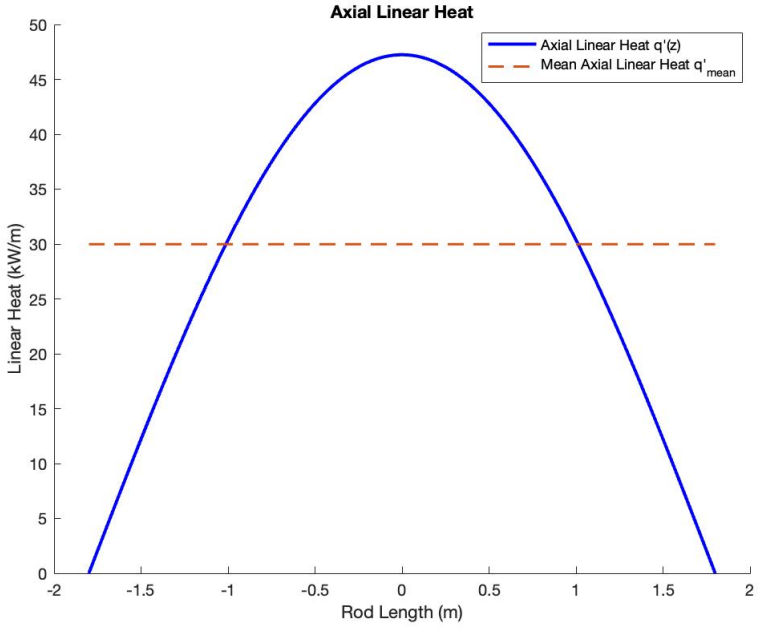

Figure 3: Axial linear heat profile

averaged. Reminding the form of the adimensional parameters :

$$Re = \frac{GD_{hyd}}{\mu}, \qquad Pr = \frac{\mu c_p}{k}, \qquad Nu = \frac{\alpha D_{hyd}}{k} \tag{2}$$

The correlation is given by the equation :

$$Nu = 0.023 Re^{0.8} Pr^{0.4} \tag{3}$$

2.2. Onset of Nucleate Boiling

The ONB correlation used is the one suggested by **Frost-Dzakowic**, which consists in the **Davis-Anderson** correlation refined with a corrective factor accounting for the flow of the fluid : the Pr_l . The equation is the following :

$$\Delta T_{w,ONB} = \sqrt{\frac{8\sigma q'' T_{sat}}{k h_{lg} \rho_g}}\ Pr_l \tag{4}$$

Where, h_{lg} stands for the transition (liquid to gaseous) enthalpy , and $\Delta T_{w,ONB}$ for $(T_w - T_{sat})$ at the onset of nucleate boiling point.

2.3. Subcooled Boiling

For this particular heat transfer condition different approaches, and hence correlations, were used in the simulations. The two most relevant ones for the case study are here described.

2.3.1 Bjorge, Hall and Rohsenow superposition method

Bjorge, Halll and Rohsenow proposed a non-linear superposition to produce an heat flux relation for the subcooled boiling region. It actually consider the contribute of both the convective and the nucleate boiling heat transfer in the following way :

$$q''^2 = q_c''^2 + (q_{nb}'' - q_{ONB}'')^2 \tag{5}$$

Where q_c'' represents the convective heat transfer contribution calculated also in this case with the **Dittus-Boelter** correlation, q_{nb}'' the nucleate boiling contribution and q_{ONB}'' the value obtained by the nucleate boiling correlation selected in the ONB point. To better visualize it, can be written the expanded form for the formula:

$$q''^2 = \alpha_{lo}^2 (T_w - T_{b,z})^2 + (C_b (T_w - T_{sat})^n - C_b \Delta T_{w,ONB}^n)^2 \tag{6}$$

Where the boiling coefficient C_b and the exponential term n can be extrapolated by a generic nucleate boiling correlation as : $q'' = C_b(T_w - T_b)^n$. To apply this method three different nucleate boiling correlations were used:

- The **Jens-Lottes** correlation, which has a pressure range of applicability of 0.7-17.2 MPa, and the equation expressed in $\frac{MW}{m^2}$, MPa and $°C$.

$$q''_{nb} = \frac{e^{\frac{4P}{6.2}}}{25^4}(T_w - T_{sat})^4, \qquad \text{with :} \qquad C_{b_{JL}} = \frac{e^{\frac{4P}{6.2}}}{25^4}, \qquad n = 4 \tag{7}$$

- The **Thom** correlation, which has a pressure range of applicability of 5.17-13.79 MPa, and the equation expressed in $\frac{MW}{m^2}$, MPa and $°C$.

$$q''_{nb} = \frac{e^{\frac{2P}{8.7}}}{22.7^2}(T_w - T_{sat})^2, \qquad \text{with :} \qquad C_{b_{Th}} = \frac{e^{\frac{2P}{8.7}}}{22.7^2}, \qquad n = 2 \tag{8}$$

- The **Rohsenow** correlation :

$$q''_{nb} = \mu_l h_{lg}\sqrt{\frac{g(\rho_l - \rho_g)}{\sigma}}\,(\frac{c_{p,l}}{C_{sf}h_{lg}Pr_l})^3(T_w - T_{sat})^3, \tag{9}$$

$$\text{with :} \qquad C_{b_{Roh}} = \mu_l h_{lg}\sqrt{\frac{g(\rho_l - \rho_g)}{\sigma}}\,(\frac{c_{p,l}}{C_{sf}h_{lg}Pr_l})^3, \qquad n = 3 \tag{10}$$

  Where the fluid properties are evaluated at saturated condition, and the parameter C_{sf} takes into account the liquid- surface contact type, with the value for water flowing over stainless steel taken from experimental tables : $C_{sf} \sim 0.0132$.

2.3.2 Liu-Winterton correlation

Liu and Winterton proposed on Ref. [7] a new type of subcooled boiling correlation based on the previous work over the flow boiling heat transfer made by **Chen**. The proposed correlation is :

$$q'' = \sqrt{(F\alpha_{lo}\Delta T_{w,b})^2 + (S\alpha_{nb}\Delta T_{w,sat})^2} \tag{11}$$

Where $\Delta T_{w,b}$ is $(T_w - T_b)$ and $\Delta T_{w,sat}$ is $(T_w - T_{sat})$. Also in this model, the α_{lo} is calculated using the **Dittus-Boelter** correlation, while for the nucleate boiling heat transfer coefficient α_{nb} is used, like suggested by **Liu and Winterton** themselves, the **Cooper** correlation :

$$\alpha_{nb} = 55p_r^{0.12}q''^{2/3}(-\log_{10} p_r)^{-0.55}M^{-0.5} \tag{12}$$

With M the molar mass of water.
The value of the coefficient F is set to 1 , while the value of the coefficient S is given by :

$$S = (1 + 0.55Re_{lo}^{0.16})^{-1} \tag{13}$$

As suggested in Ref. [7], when the temperature is unknown, introducing the coefficients :

$$A_{bp} = \frac{\alpha_{lo}}{S\alpha_{nb}}, \qquad A_{qp} = \frac{q''}{S\alpha_{nb}(T_{sat} - T_b)} \tag{14}$$

Both the wall temperature and the heat transfer coefficient can be found simply by using the set of equations given by :

$$\begin{cases} \Delta T_{w,b} = \dfrac{T_{sat} - T_b}{1 + A_{bp}^2}\left[1 + \sqrt{1 + (1 + A_{bp}^2)(A_{qp}^2 - 1)}\,\right] \\ \alpha_{tp} = \dfrac{q''}{\Delta T_{w,b}} \end{cases} \tag{15}$$

And obviously α_{tp} is the two-phase heat transfer coefficient.

2.4. Saturated Boiling

The analysis of the saturated boiling starts when the average bulk temperature is equal to the saturated one, and lasts up to the end of the channel if no boiling crisis condition is reached. For the case study two different approaches were adopted.

2.4.1 Kandlikar correlation

On his paper published on 1990 (Ref. [4]) **Kandlikar** proposed a correlation for the saturated two phase flow which is based on the previous study made by **Shah** but with a much larger data set this time. The final form of the correlation proposed is :

$$\frac{\alpha_{tp}}{\alpha_l} = c_1 Co^{c_2} (25 Fr_{lo})^{c_5} + c_3 Bo^{c_4} F_{fl} \tag{16}$$

Where the variables are given by :

$$Bo = \frac{q''}{G h_{lg}}, \qquad Co = \left(\frac{1-x}{x}\right)^{0.8} \left(\frac{\rho_g}{\rho_l}\right)^{0.5}, \qquad Fr = \frac{G_l^2}{\rho_l^2 g D_{hyd}} \tag{17}$$

Kandlikar himself suggestd to estimate the convective heat transfer coefficient α_l (liquid *alone*) using the **Dittus-Boelter** correlation. The values of the parameters c_i are tabulated in Ref. [4] and are strictly dependent on the type of dominant physical phenomenon on the global two-phase heat transfer coefficient. Experimentally they are estimated to be respectively :

Kandlikar propose for the Constants		
Constant	*Convective Region*	*Nucleate Boiling Region*
$\boldsymbol{c_1}$	1.1360	0.6683
$\boldsymbol{c_2}$	-0.9	-0.2
$\boldsymbol{c_3}$	667.2	1058.0
$\boldsymbol{c_4}$	0.7	0.7

Table 1: Ref. [4] proposed coefficients for eq. 16

And the value of the coefficient $\boldsymbol{c_5}$ in this case study is set equal to zero being a vertical flow. Putting also the value of F_{fl} equal to one (observed experimentally for water), the final correlation has two different forms, one relative to the *convective dominated* region, and the other to the *nucleate boiling dominated* one :

$$\begin{cases} \textbf{C.D. :} & \alpha_{tp_{C.D.}} = & \left(1.136 Co^{-0.9} + 667.2 Bo^{0.7}\right) \alpha_l \\ \textbf{N.B.D. :} & \alpha_{tp_{N.B.D.}} = & \left(0.6683 Co^{-0.2} + 1058 Bo^{0.7}\right) \alpha_l \end{cases} \tag{18}$$

In the end the heat transfer coefficient for the saturated boiling region is simply given by the maximum value within the two calculated in eq. 18 :

$$\alpha_{tp} = \text{Max}(\alpha_{tp_{C.D.}}, \alpha_{tp_{N.B.D.}}) \tag{19}$$

In addition of being a very simple correlation and being validated with good experimental results, it offers also a relatively smooth transition from the *nucleate boiling dominated* region to the *convective dominated* region.

2.4.2 Ağlar correlation

In 2018 in Ref. [1] **Ağlar** proposed a new correlation, based on the previous studies made by **Chen, Shah, and Gungor-Winterton**. The two-phase heat transfer coefficient is described only as a macroscopic parameter. Considering the different behaviour of both the velocity and temperature profile during the saturated flow boiling, an enhancement factor proposed, called E_{aglar}, depending on both the ratios of the Reynolds' and Prandtl' numbers of the two-phase and liquid alone cases :

$$\begin{cases} E_{aglar} = \left(\dfrac{Re_{tp}}{Re_l}\right)^X \left(\dfrac{Pr_{tp}}{Pr_l}\right)^Y \\ \alpha_{tp} = E_{aglar} \alpha_l \end{cases} \tag{20}$$

With X and Y unknown variables, and α_l the liquid *alone* heat transfer coefficient calculated with a single phase flow correlation (**Dittus-Boelter**). The first ratio, the Reynolds numbers one, following the suggestions of previous studies, assumes the form :

$$F = \left[1 + c_1 Bo^m + c_2 \left(\frac{x}{1-x}\right)^n \left(\frac{\rho_l}{\rho_g}\right)^z\right]^p \tag{21}$$

While the ratio between the Prandtl numbers, assuming the validity of the **Colburn** analysis extendable also to the two-phase flows, could be rewritten as :

$$A = \left[\frac{f_{tp}}{f_l} \left(1 + \frac{c_{p,g}}{c_{p,l}} \frac{x}{1-x} \right) \right]^r \tag{22}$$

The two-phase and liquid *alone* friction factors are calculated with the instructions given in Ref. [1] . Having in the present study always Reynolds numbers over the threshold set at 3000 , then the formulas become :

$$\begin{cases} f_{tp} = 0.014 + (0.125/Re_{tp}^{0.32}) \\ f_l = 0.014 + (0.125/Re_l^{0.32}) \end{cases} \tag{23}$$

With the Reynolds numbers calculated as :

$$Re_l = \frac{D_{hyd} G (1-x)}{\mu_l} \quad \longrightarrow \mu_l : \text{liquid viscosity} \tag{24}$$

$$Re_{tp} = \frac{D_{hyd} G}{\mu_b} \quad \longrightarrow \mu_b : \text{mean two-phase bulk viscosity} \tag{25}$$

And the mean two-phase bulk viscosity using the **McAdams** correlation as :

$$\frac{1}{\mu_b} = \frac{x}{\mu_g} + \frac{1-x}{\mu_l} \tag{26}$$

In the end, considering the tabulated values for the constants previous introduced, the form of the **Ağlar** correlation can be visualized as :

$$\alpha_{tp} = \left[1 + 3650 Bo^{0.83} + 0.31 \left(\frac{x}{1-x} \right)^{0.8} \left(\frac{\rho_l}{\rho_g} \right)^{0.68} \right]^{1.01} \left[\frac{f_{tp}}{f_l} \left(1 + \frac{c_{p,g}}{c_{p,l}} \frac{x}{1-x} \right) \right]^{0.82} \alpha_l \tag{27}$$

The strength of this correlation for the case study lays on the fact that it is developed using data sets well within the ranges considered for this simulation, and seems to have one of the best behaviours dealing with water in vertical flows.

2.5. Critical Heat Flux

For the treatment of the Critical Heat Flux were used two different models : the **CISE-4** and the **Groenveld** correlations.

2.5.1 CISE-4

This correlation was developed following the concept of boiling length-quality relation and is restricted to BWR application to describe the **Dryout** phenomenon. The correlation calculates the critical quality (x_{cr}), that is the quality for which level is reached the critical condition. For our purposes, the correlation can be rewritten in the form :

$$x_{CHF} = \frac{a L_b}{L_b + b} \tag{28}$$

Where L_b is the boiling length, which is defined as the distance from zero equilibrium quality to the end of the channel, the coefficients a and b are given by:

$$\begin{cases} a = \dfrac{1}{1 + 1.481 \times 10^{-4} (1-p_r)^{-3} G} & \text{if } G < G_{ref} \\ a = \dfrac{1-p_r}{G/1000}^{1/3} & \text{if } G \geq G_{ref} \end{cases} \tag{29}$$

With the G_{ref} being the reference mass flux given by : $G_{ref} = 3375(1-p_r)^3 [\frac{kg}{m^2 S}]$. In the end, the coefficient b given by :

$$b = 0.199 (p_r^{-1} - 1)^{0.4} G D_{hyd}^{1.4} \tag{30}$$

All the correlation uses the I.S. of measure , and has a perfect range of applicability for this case study being developed for BWRs.

2.5.2 Groenveld's Lookup-Table

The **Groenveld correlation** can be used with good accuracy for both the **Dryout** and the **Departure from Nucleate Boiling** phenomena. Has one of the widest range of applicability within the CHF models, and is based on the *Groenveld's Lookup Table* , basically a normalized set of data relative to a 8mm water cooled vertical tube. The correlation returns the estimated critical heat flux calculated starting from the data bank of heat fluxes in the lookup table and applying corrections to them through different coefficients, each one related to a peculiar characteristic of the system considered. The correlation has the form :

$$q''_{CHF} = (q''_{CHF})_{L.U.T.} K \tag{31}$$

In the numerical simulation on Matlab the code available on Ref. [2] on GitHub was used. The corrective coefficients exploited are two :

- K_1 : *Rod diameter factor* , obtained as :

$$\begin{cases} K_1 = (8/D_{hyd})^{0.5} & \text{for : } 3 < D_{hyd} < 25mm \\ K_1 = 0.57 & \text{for : } D_{hyd} > 25mm \end{cases} \tag{32}$$

- K_4 : *Heated length factor* , obtained as :

$$K_4 = e^{\frac{D_{hyd}}{L} exp(2\alpha_{HEM})}, \quad \text{where : } \alpha_{HEM} = \frac{x\rho_l}{x\rho_l + (1-x)\rho_g} \tag{33}$$

And so, in the end the correlation becomes :

$$q''_{CHF} = (q''_{CHF})_{L.U.T.} K_1 K_4 \tag{34}$$

3. Numerical Simulation Results and Discussion

The numerical simulations' results and the related discussions are divided in two different parts: the first, dealing with the complete characterization of both the wall temperature and the heat transfer coefficient at nominal power condition, and the second part devoted to make an in depth characterization of the Thermal crisis phenomena involved in a BWR.

3.1. Nominal Condition : Wall Temperature and Heat Transfer Coefficient Analysis

The steps followed in the simulation are the ones illustrated in fig.4. A discretization is made all along the length of the fuel rod, dividing it in segments of 1 mm. The inlet conditions are imposed. The simulation can be subdivided in different steps : first there is the calculation of the wall temperature and of the heat transfer coefficient up to the onset of nucleate boiling conditions; then the same process is made for the subcooled flow boiling, with the limit condition being this time the saturation temperature of the coolant; last but not least there's the simulation of the flow boiling in saturated condition, which lasts up to the end of the rod. It must be underlined that the discussion of the critical condition is not made in this section (obviously while making the calculations on MATLAB, was checked that the critical heat flux was not reached up to the end of the rod). Before watching the results, must be also precised the energy balances used through all the simulation. Calling as Q_{bin} the heat exchanged within each segment (z_i, z_{i+1}) the equations used, together with the ones presented in section 2 , are :

$$T_{b,@z_{i+1}} = \frac{Q_{bin}}{m\ c_{p_l}} + T_{b,@z_i}; \tag{35}$$

$$\Delta x = \frac{Q_{bin}}{m\ h_{lg}}. \tag{36}$$

The first equation is used up to the saturation condition, while the second one is used from the saturation condition up to end, and represents the increase of the average vapour quality in the i-th considered segment.

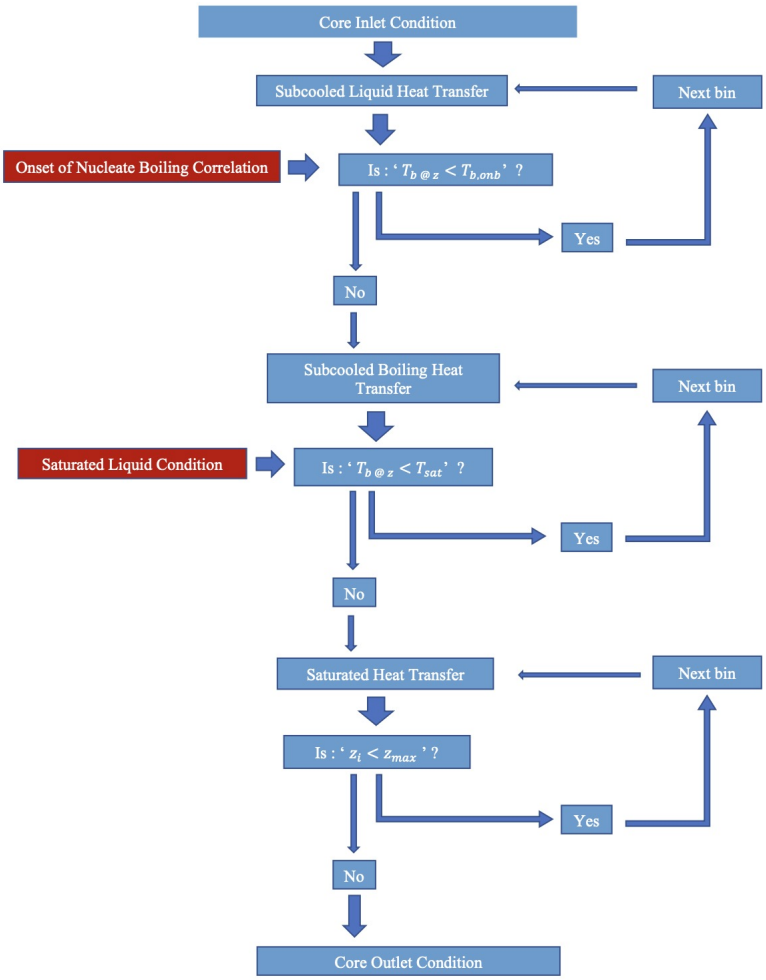

Figure 4: Logical steps followed for the numerical simulations

Lets now pass to the numerical results. On fig.5a and fig.5b are presented the plots obtained with the analysis of the *subcooled liquid* and *subcooled flow boiling* zones.

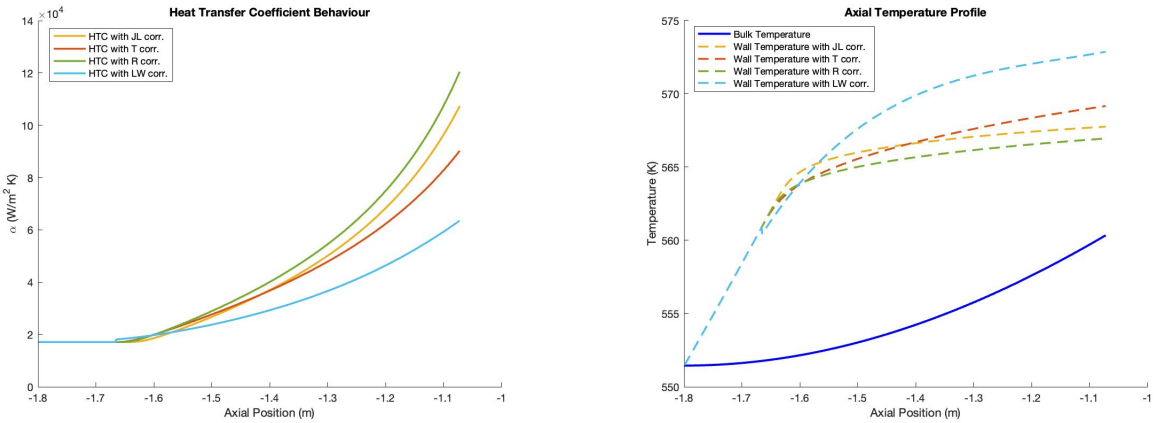

(a) (b) .

Figure 5: Subcooled liquid-boiling Heat Transfer Coefficients (a) and Temperature profiles (b)

In the first part of fig. 5a , the *subcooled liquid* zone, the profile of the heat transfer coefficient (abbr. HTC) is roughly constant: the increase due to the higher c_p of water at higher temperatures is so small that it cannot be appreciated on this graph. The enhanced heat transfer condition starting from the *onset of nucleate boiling* (estimated from the simulations at: $z_{ONB} = -1.667$ m) on the other hand is clearly visible: the HTC has

a fast boost, becoming in only half a meter several times the one at inlet conditions. The behaviour of the coefficient is obviously reflected in the temperatures' profile in fig. 5b: in the first part, up to the ONB, the temperature difference between the water and the wall increases a lot, as the water is not able to remove heat in an efficient way; then from the ONB to the *saturated liquid* condition (estimated at $z_{sat} = -1.073$ m) are graphed the different shapes of the four correlations adopted in the discussion, and can be seen that for each one the *subcooled flow boiling* condition contribute to reducing the temperature gap between the coolant and the wall previously created. The three correlations using the *Bjorge-Hall-Rohsenow superposition method* give higher esteems of HTC with respect to the one given by the *Liu-Winterton correlation*. The difference between one correlation and the other is not so small, especially if are considered the two extreme ones: the *Rohsenow* and the *Liu-Winterton*. In fact, the first esteems the HTC to be roughly 2 times the one predicted by the second cited correlation, and having as a consequence a difference in the wall temperature profile of ~ 6 deg. Similar observations could be made also for the *Thom* and *Jens-Lottes* correlations, but not so pronounced, having these two what can be considered a sort of 'intermediate behaviour', less conservative than the *Liu-Winterton* one, and less optimistic than the *Rohsenow* approach. Making these first considerations, can be now analyzed the complete temperature and HTC profiles over the entire length of the rod.

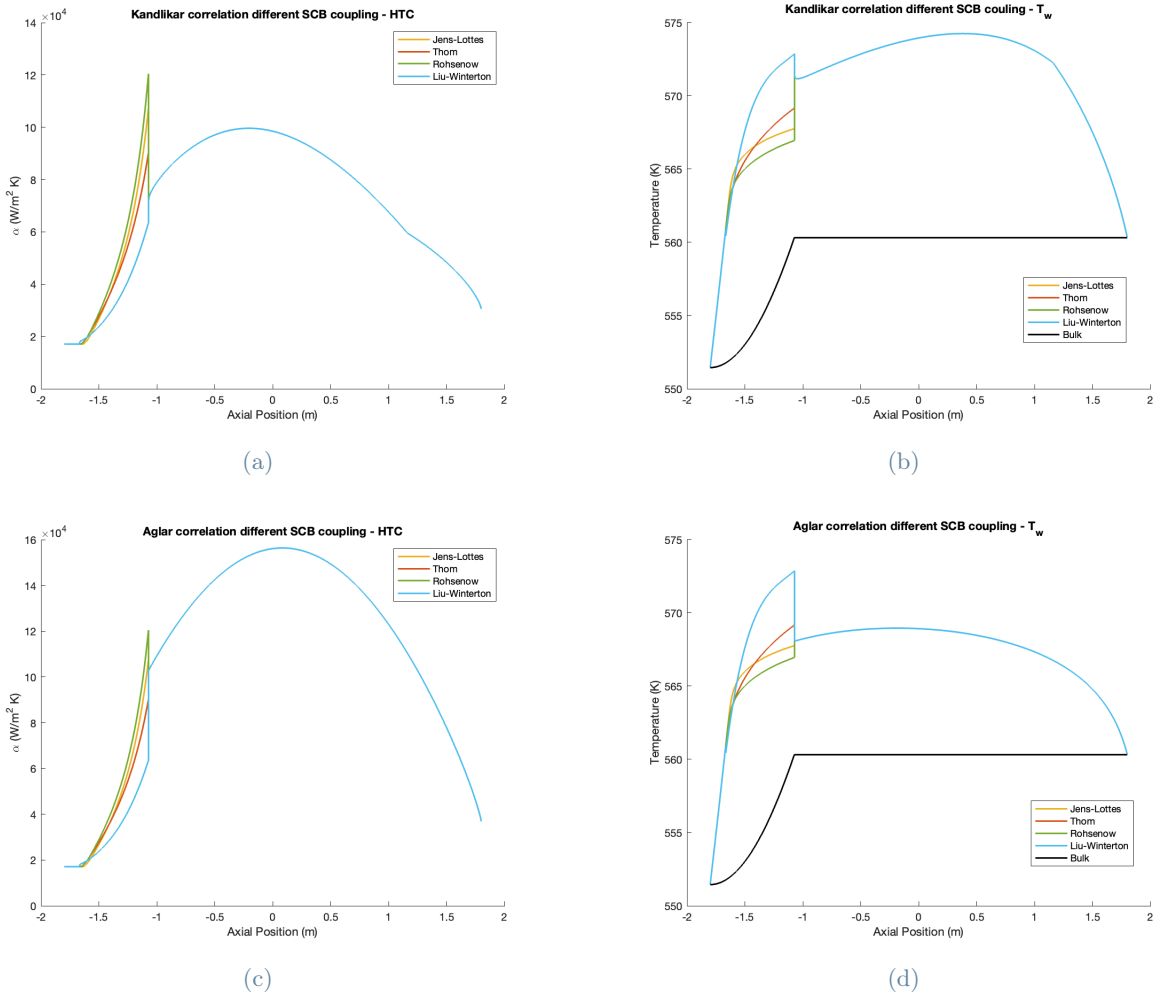

Figure 6: Different Subcooled Boiling - Saturated Boiling correlations coupling

It's immediate to see that in the *saturated boiling* region the adoption of the *Ağlar* correlation gives an esteem of the HTC much higher than the one offered by the *Kandlikar's*. Between these two can be individuated mainly three differences: firstly the magnitude of the HTC that is increased, passing from the *Kandlikar* to the *Ağlar* model of $\sim 60000 \frac{W}{m^2 K}$ at the maximum point; then can be denoted the smooth continuous curve of fig. 6c on the contrary to what is found in fig. 6a, where the passage from the boiling to the convective dominated zone as expressed in eq. 18 is clearly visible; last but not least the position of the peak (maximum HTC) in the *Ağlar* correlation is perfectly in the midpoint of the rod, at the heat flux maximum level, while in the *Kandlikar* correlation is situated in the first part of the rod, roughly half a meter from the center. After underlining these differences, the main point of the discussion now is what couple of correlations would be the most suitable one

dealing with this case study, or in other words what couple of *saturated-subcooled boiling correlations* makes sense to use together to predict the temperature and HTC profiles in this approximated model of a BWR fuel rod. To answer this question some considerations about the obtained results must be pointed out. From what is seen up to now, we can actually categorize the different models as *overestimating* or *underestimating* correlations. However all of them were selected considering a good fitting with the problem technical parameters, and in addition, some also represent different approaches to the same starting models (for ex. the *Kandlikar* and the *Ağlar* on *Chen*'s model). Furthermore being all produced empirically by collecting experimental data and using a parametric description, they are all intrinsically characterized by an error. Thus, watching the very different results obtained using one or the other, would be much wiser to not select only one model to describe the heat transfer phenomena, coming to the compromise of giving an **upper** and **lower** bound for both the HTC and the wall temperature. Turning the discussion in this direction, on one side we would actually fail in giving a detailed description of the two variables, but on the other hand important results could be anyway achieved: first, would be provided reliable upper and lower ranges for a first approximation quick analysis of the heat transfer mechanisms characteristic parameters at nominal condition; and secondly, is not given a fanciful ´one model' description without actually having true motivations for selecting one correlation instead of the others as, although some correlations could have a better data set for this case study (considering the one from which they were developed), only a detailed experimental analysis could remove every doubt. Having made these considerations, can be now discussed the proposed correlation for the already cited **upper** and **lower** bounds. Considering the HTC, looking at the results of the numerical simulations of the *saturated* zone, the conclusion is almost obvious: while the *Kandlikar* approach represents the more conservative one between the two, the Ağlar approach (*note*: based on data on average more similar to this case study) is much more optimistic. In reverse, the *subcooled boiling* region has not a discussion as simple as this. Beginning with the *Kandlikar* correlation, thus the **lower** bound in terms of HTC, the choice on which *subcooled* model couple it with naturally falls on one between the *Liu-Winterton* and the *Thom* correlations. The first in the end is the selected one: it represents the ´minimum' esteem in terms of HTC, having at the same time the peak wall temperature not so high to overcome the one calculated by the saturated boiling correlation and the discontinuity in the temperature profile pretty similar, actually lower, to the one predicted by the *Thom* correlation. Passing on the choice of which model should be coupled with the Ağlar one, is evident the exclusion of the previously cited *Liu-Winterton* and *Thom*: selecting the upper bound of the HTC would be preferable, looking to the axial wall temperature, to select an optimistic scenario such that the highest estimated temperature is the one calculated by the *saturated* boiling condition, and not by the *subcooled* one. Within the remaining two, the *Rohsenow* and the *Jens-Lottes* correlations, the choice falls on the second one. The motivation stands on the fact that regarding the HTC profile, the saturated region is by far the dominating one (the α is $\sim 40000 \frac{W}{m^2 K}$ over the subcooled region, regardless of which one is selected) and making a pick between these two is not as relevant as the exclusion of the previous two correlations. On contemporary, looking at the temperature profile, both are below the temperatures predicted in the saturated region with a very small difference. The selection of the *Jens-Lottes* thus is actually made due to the smoother transition and lower discontinuity offered passing to the *saturated boiling*. In the end, are in this way obtained :

- The **HTC Upper Bound - (Optimistic scenario)** : *Jens-Lottes/Ağlar* correlations;
- The **HTC Lower Bound - (Pessimistic scenario)** : *Liu-Winterton/Kandlikar* correlations.

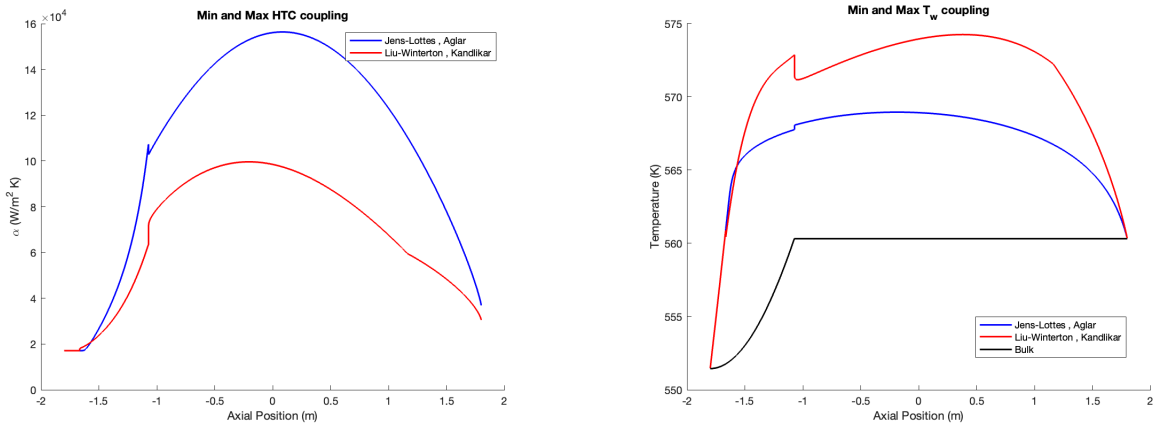

(a) (b)

Figure 7: Proposed HTC (a) and Wall Temperature (b) lower and upper bounds

NOTE: As written in the last two lines, the **upper** and **lower** bounds are related respectively to **optimistic** or **pessimistic** scenarios because of the different esteem given of the HTC : the first, on the contrary of the second, evaluates a good heat removal efficiency, leading thus to better (optimistic) global thermal conditions.

More quantitative data from the numerical simulation can be observed in the table below, where are reported the maximum values of the *wall temperature* and *HTC* for both the **Upper Bound (U.B.)** and the **Lower Bound (L.B.)**.

Maximum values of HTC and Wall Temperature							
$\alpha_{U.B._{max}}$	$156380 \frac{W}{m^2 K}$	$T_{wU.B._{max}}$	568.9593 K	$\alpha_{L.B._{max}}$	$99623 \frac{W}{m^2 K}$	$T_{wL.B._{max}}$	574.2564 K

3.2. Critical Heat Flux in BWRs : Thermal Crysis' Characteristics and Dryout Sensitivity Analysis

3.2.1 BWRs CHF Phenomenological Analysis

BWRs, like all the flow boiling operating technologies, could be characterized by two different types of phenomena approaching the *Critical Heat Flux*: the **Departure from Nucleate Boiling**, and the **Dryout**. While the DNB is a local condition, whose reference indicator is the local heat flux ratio (also called DNBR), the Dryout is dependent on the channel history, thus on the channel power, with the indicator being the **Critical Power Ratio (CPR)** , defined as 'the ratio between the power of the channel in critical condition and the power in nominal condition', as suggested in Ref. [6]. The two phenomena are both intrinsically different one from the other: one is local, while the other is global; one is characterized by low qualities at the CHF occurrence (DNB) , while the other by high qualities (Dryout); in one case the limits are typically given in terms of CHFs (DNB), while in the other by global parameters like the Critical Quality (x_{cr} , the vapour quality reached at the insurgence of critical conditions). On the other hand in BWRs, the high quality operational conditions, together with the low heat flux in zones where the quality is low (at the entrance), suggests in normal conditions the need of having a reliable correlation to ensure that the upper part of the cladding is wetted by the liquid, without undergoing Dryout. A graphical and numerical evaluation of why BWRs are either characterized by Dryout limits than DNB's ones is here presented.

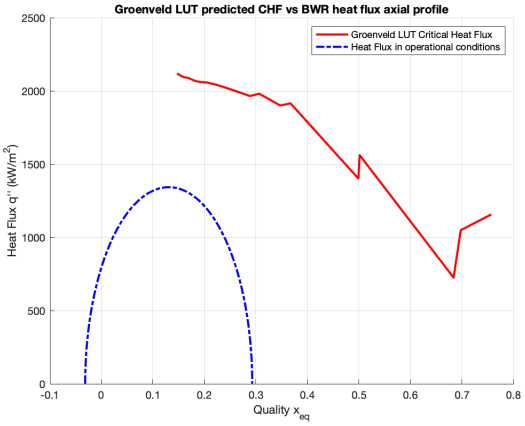

Figure 8: Groenveld LUT CHF profile compared to the channel nominal heat flux profile.

Groenveld's correlation, as explained in subsection 2.5.2 , is a general correlation predicting both DNB and Dryout conditions. Here in fig. 8 is plotted (using Ref. [2] GitHub repository's MATLAB code) the CHF in function of the quality, together with the heat flux-vapour quality curve related to the channel. Important considerations from a qualitative point of view can be carried out. Considering both the mass and the pressure fixed parameters, then the curve related to the lookup-table (**LUT**) and the entrance quality point, will be fixed as well. Considering a change of the heat flux on the rod, for example due to the extraction of some control rods contemporary, then the blue curve will tend both to increase its height, but also its extension to the right side of the graphic. This actually is translated to the fact that, provided the necessary pressure and mass flow conditions which are the typical operational ones, the intersection of the two curves appears to be at relatively high quality, leading to the *Dryout*, and not to the DNB. Detailed studies about this concept were made, and concerning one of them dealing with BWRs, in Ref. [6] is underlined a lower bound for the critical quality in order to give life as a thermal crisis phenomenon the *Dryout*: $x_{cr,dryout\ L.B.} \sim 0.325$. For this case study this

approach with *Groenveld's LUT*, together with the discussions made on Ref. [6] were considered sufficient in order to pass to characterize with a more detailed approach the CHF in operational condition only looking to the Dryout global phenomenon.

3.2.2 Dryout Sensitivity Analysis in Steady State Operational Conditions

The correlation used to describe the behaviour of the Dryout occurrence in different conditions is the **CISE-4**, presented in 2.5.1 . Giving it as an output the critical quality x_{cr} , the related critical heat parameters were extracted considering the limit condition in which the insurgence of the critical quality is at the exact end of the rod. With some mathematical manipulation can be found the equations :

$$q'_{0,CHF} = \frac{m\pi}{2L_{rod}}(h_{sat} - h_{in} + x_{cr}h_{lg}) \tag{37}$$

$$Q_{CHF} = \int_{-L_{rod}/2}^{L_{rod}/2} q'_{0,CHF}\cos(\frac{\pi x}{L_{rod}}) \tag{38}$$

Where Q_{CHF} indicates the critical thermal power of the rod to incur in the Dryout in the final point of the channel. The calculation of the CPR is then simply :

$$CPR = \frac{Q_{CHF}}{Q_{nominal}} \tag{39}$$

Developing in this way the code, for the parameters taken into account in the analysis, which correspond to a steady state 100% nominal power of the reactor, the results are the following :

Nominal Condition Dryout-related Parameters					
x_{cr}	0.4007	Q_{CHF}	144.2516 kW	CPR	1.3324

Which actually is a pretty good safety margin (Note that to **not** be in Dryout condition the value of the CPR, from the definition, must overcome 1). These parameters can be better comprehended looking to the vapour quality profile, and specifically to the value at the exit, which only nearly reaches the 0.3 (fig. 9).

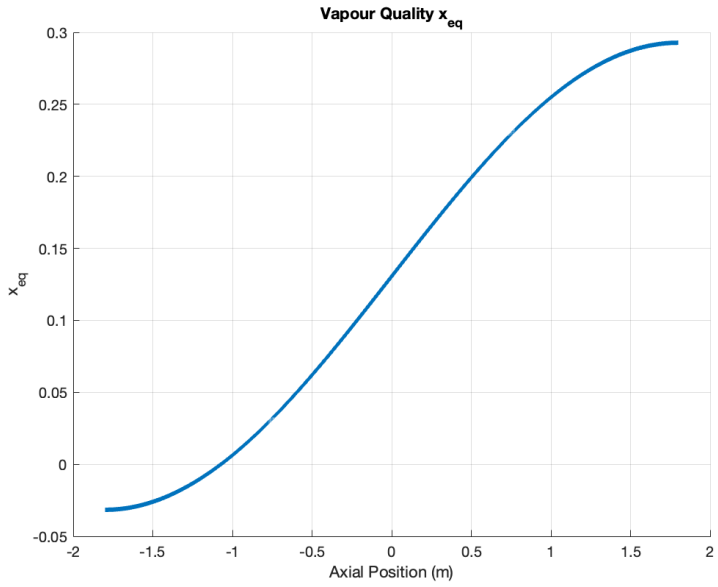

Figure 9: Reactor nominal power vapour quality axial profile

More interesting conclusions can be then obtained by looking at the results of the *Dryout sensitivity analysis*. Using another time the *CISE-4* correlation and eq.37-38 , and making an iterative code over both the mass flow rate and the rod thermal power, could be found the values of x_{cr} and CPR in what can be considered to be different operational conditions possibilities.

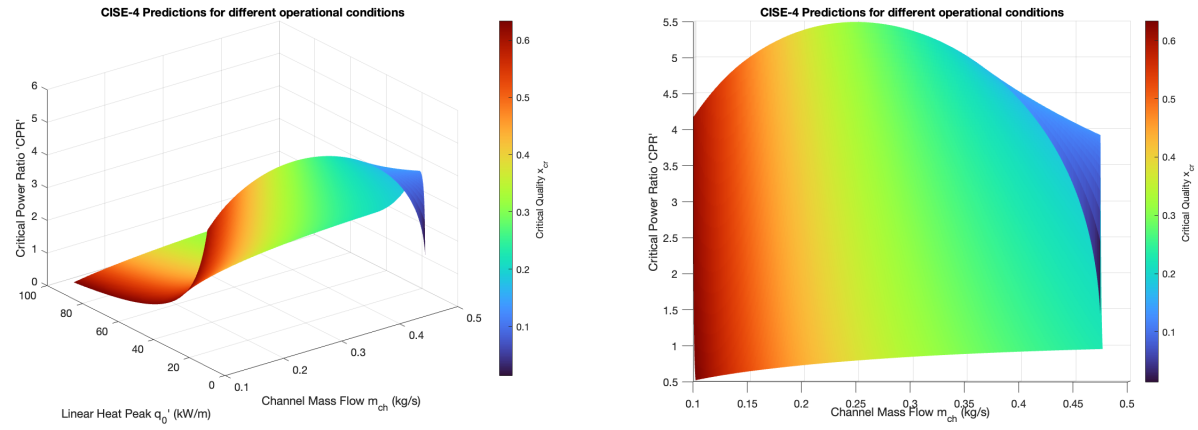

(a) (b)

Figure 10: CISE-4 Dryout sensitivity analysis (1)

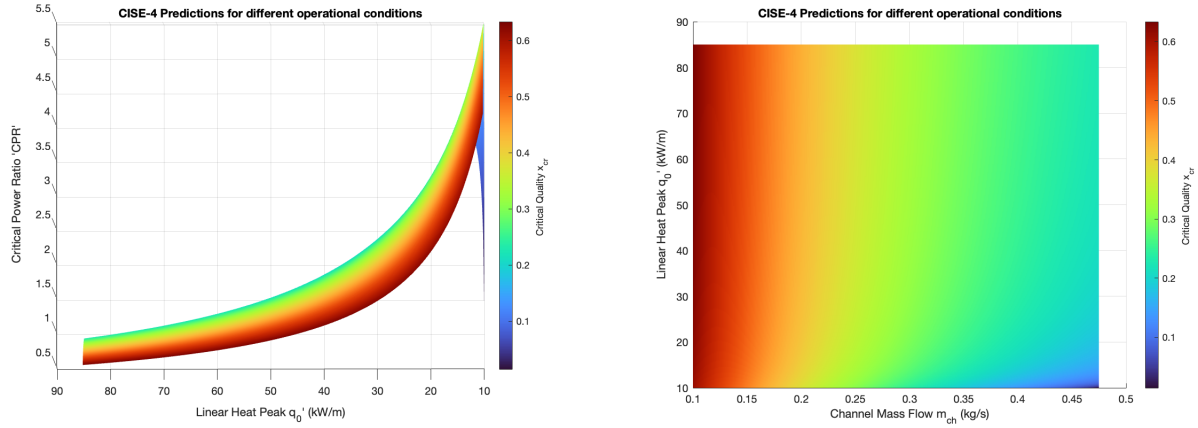

(a) (b)

Figure 11: CISE-4 Dryout sensitivity analysis (2)

Starting looking to fig. 11(b) , can be visualized the behaviour of the x_{cr} . The results are in accordance with the correlation, as the CISE predicts a behaviour of the critical quality such that decreasing the mass flux the value of x_{cr} approaches one. The effect of increasing the heat power of the channel is more visible in the intermediate mass flow region, where a higher power leads to a higher boiling length L_b, which inserted in eq. 28 has the global effect to increase the critical quality. The behaviour of the CPR can be then visualized using fig. 10(b)-11(a) . In the second (fig. 11(a)) the behaviour is simple: the critical heat flux (and so the power) is set by operational conditions like the mass flux and the pressure of the system, the effect of decreasing, taking the other parameters as fixed, the rod heat flux is only the one of increasing the CPR as the condition is further and further from the critical one like suggests eq. 39 . On the other hand explaining the curve shape within the change of the mass flow is not so straight on, but can be given some physical interpretations. Looking to fig. 10(b) can be seen the profile of the surface with $q'_{0,min}$ (the one below) and with $q'_{0,max}$ (the one above). Both express the dependence of the CPR on the mass flow, but at different levels of thermal power. The general behaviour suggested by them is the one leading to a more accentuated parabolic form of the surface with $q'_0 \to 0$. This actually means that the maximum of the CPR at a certain point will no more be at the border, and will gradually move to the central part of the surface increasing the power. The increase of the CPR with the mass flow, at a given q'_0 , can be physically interpreted simply by the fact that by increasing the mass flow the heat exchange conditions are gradually improved, moving from a zone where the Dryout was reached ($CPR < 1$), or where was not so high, to higher CPR , safer, zones. On the other hand, where the formation of the maximum point is in the middle of the surface plot, from that point toward higher mass flow zones, cannot be given a real physical explanation. The most accredited explanation is a crisis of the **CISE-4** in those zones. Looking at the joint behaviour of both the Critical quality and the Critical power ratio, the maximum on fig. 10(b) of the two extremes profile is situated on both cases around a value of $x_{cr} \sim 0.3$. How

explained in 3.2.1 the Dryout condition appears when we are situated in conditions in which the critical quality is pretty high. Thus, the *Dryout* lower bound previously presented of $x_{cr} \sim 0.325$ approximately corresponds to the point of maximum in the parabolic shape that can be individuated in the curve. This not only explains the parabolic trend, but also the strange conformation assumed by the surface at low heat and high mass flux limit conditions, in which the **CISE-4** is no more a good CHF indicator. In the end, discarding the results with a critical quality $x_{cr} < 0.325$, are obtained in first approximation reliable results of different possible operational conditions limits of a BWR fuel rod. The effort of this analysis stands also in the fact that typically the power excursion of a reactor in normal conditions is made by setting first of all the operational desired pressure and mass flow, to then extract the control rods and regulate the fuel rods' thermal power through the neutronic; thus these conditions are the ones plotted in figures 10-11 with a mass flow typically set around 0.2 kg/s, making in normal conditions the BWR's power excursion approachable with a *Dryout* model, thus with the described model. Surely, in accidental conditions the situation would be completely different, and a DNB model would have also to be taken into consideration.

Conclusions

In Conclusion, the analysis made can be considered to have satisfactory results: the output parameters and global trends fall all within the characteristics range for BWRs (present in Ref. [6]) and they all have a physical background. Surely a lot of simplifications were made in all the assumptions for the case study :

- The cosinusoidal power profile is a simplification of the real one, which would be slightly deformed, and that would have to take into account also the neutronic, especially for the entrance and exit power. For the analysis was considered a restriction of the neutron transport zone to merely the length of the fuel rod;
- A more realistic description of a reactor core heat transfer phenomena would have to take into account the entire assembly, with all the mixing phenomena within one flow area and the other;
- A global description of the reactor core should also consider the different power of one rod with respect to the other. For this paper was only considered an average rod's power;
- The use of correlations not directly developed to be used for this type of technology, together with also the use of numerical MATLAB simulations, lead to the presence of an intrinsic error in the results.

On the other hand were achieved interesting goals: reliable ranges in nominal power condition for both HTC and wall temperature were given, together with a sensitivity analysis that seems to describe in a good way the thermal crisis occurrence of a single fuel rod. To sum up all: the description of the thermal phenomena occurring inside the core of a nuclear reactor is surely a very complex field of study, which would need the maximum effort in describing all with as much accuracy as possible. This study shows that with a bit of effort on the other hand, without too much complex simulations, pretty good approximated results can be achieved.

Notes

This paper was entirely developed by me, **Davide Marchesi**, within the project for the exam of *Multiphase Systems and Technologies* of Professor **Colombo Luigi P.M.** at **Politecnico di Milano**. All the material used to develop this research was cited in the *References* part. In addition to this, all the code used by me is open source and viewable on my GitHub repository at the following url: https://github.com/davidemarchesi/BWR_SS_thermal-analysis . Here can be directly seen the web open source references [3]-[2].

References

[1] F. Ağlar. A new heat transfer correlation for saturated flow boiling of water with prandtl number improvement. *Karaelmas Science and Engineering Journal*, 9:253–261, 2019.

[2] greenwoodms06. 2006 groeneveld critical heat flux lut, 2016.

[3] Magnus Holmgren. X steam, thermodynamic properties of water and steam., 2023.

[4] S. G. Kandlikar. A general correlation for saturated two-phase flow boiling heat transfer inside horizontal and vertical tubes. *Journal of Heat Transfer*, 112:219–228, 1990.

[5] Colombo Luigi Pietro Maria. Miscellaneous material from the course 'multiphase systems and technologies', 2022-2023.

[6] Mujid S. Kazimi Neil E. Todreas. *Nuclear Systems : Thermal hydraulic fundamentals*, volume 1. CRC press, 3 edition, 2021.

[7] R. H. S. Winterton Z. Liu. A general correlation for saturated and subcooled flow boiling in tubes and annuli, based on a nucleate pool boiling equation. *Int. J. Heat and Mass Transfer*, 34:2759–2766, 1991.